

# Crossed Molecular Beam Study on the Formation of Phenylacetylene and Its Relevance to Titan's Atmosphere

Brant Jones,<sup>†,‡</sup> Fangtong Zhang,<sup>†</sup> Pavlo Maksyutenko,<sup>†</sup> Alexander M. Mebel,<sup>§</sup> and R. I. Kaiser<sup>\*,†</sup>

Department of Chemistry, University of Hawai'i at Manoa, Honolulu, Hawaii 96822, NASA Astrobiology Institute, University of Hawai'i at Manoa, Honolulu, Hawaii 96822, and Department of Chemistry and Biochemistry, Florida International University, Miami Florida 33199

Received: December 21, 2009; Revised Manuscript Received: March 16, 2010

The crossed molecular beam experiment of the deuterated ethynyl radical ( $C_2D$ ;  $X^2\Sigma^+$ ) with benzene [ $C_6H_6(X^1A_{1g})$ ] and its fully deuterated analog [ $C_6D_6(X^1A_{1g})$ ] was conducted at a collision energy of  $58.1 \text{ kJ mol}^{-1}$ . Our experimental data suggest the formation of the phenylacetylene- $d_6$  via indirect reactive scattering dynamics through a long-lived reaction intermediate; the reaction is initiated by a barrierless addition of the ethynyl- $d_1$  radical to benzene- $d_6$ . This initial collision complex was found to decompose via a tight exit transition state located about  $42 \text{ kJ mol}^{-1}$  above the separated products; here, the deuterium atom is ejected almost perpendicularly to the rotational plane of the decomposing intermediate and almost parallel to the total angular momentum vector. The overall experimental exoergicity of the reaction is shown to be  $121 \pm 10 \text{ kJ mol}^{-1}$ ; this compares nicely with the computed reaction energy of  $-111 \text{ kJ mol}^{-1}$ . Even though the experiment was conducted at a collisional energy higher than equivalent temperatures typically found in the atmosphere of Titan (94 K and higher), the reaction may proceed in Titan's atmosphere as it involves no entrance barrier, all transition states involved are below the energy of the separated reactants, and the reaction is exoergic. Further, the phenylacetylene was found to be the sole reaction product.

## 1. Introduction

The significance of polycyclic aromatic hydrocarbons (PAHs) (organic molecules containing benzene rings) has been proven repeatedly throughout the last decades by scientifically diverse points of views. On Earth, PAHs such as benzo[*a*]pyrene and benzo[*a*]anthracene are recognized as significant health risks due to their mutagenic and carcinogen character.<sup>1,2</sup> In conjunction with soot, PAHs further play a substantial role in global warming.<sup>3</sup> Accordingly, PAHs have garnered the interest of environmental chemists and of the combustion community.<sup>4,5</sup> However, PAHs not only are prevalent on our own planet but are also believed to be present throughout the interstellar medium (ISM).<sup>6</sup> The astronomy community suggested that the out-of-plane skeleton bending modes of PAHs are responsible for the unidentified infrared (UIR) emission bands in the 15–20  $\mu\text{m}$  region ( $500\text{--}667 \text{ cm}^{-1}$ ).<sup>7,8</sup> Furthermore, the diffuse interstellar bands (DIBs)—absorption features seen in the spectra of reddened stars throughout the Galaxy extending from the ultraviolet region to near-infrared ( $50000\text{--}7150 \text{ cm}^{-1}$ )—are thought to result from large carbon molecules and/or carbon-based nanoparticles containing anywhere between 30 and several hundred carbon atoms.<sup>9–11</sup> PAHs have also garnered interest from the astrobiology community as these molecules are believed to be associated with the origin of life.<sup>12</sup> Finally, PAHs are thought to be crucial building blocks leading to the formation of the orange-reddish haze layers on Saturn's moon Titan.<sup>13–21</sup>

But how are PAHs formed in these extreme environments? Multiple experimental studies have been completed in the last

decades, where PAHs and nanosized soot particles were observed ranging from the hydrocarbon rich flame chemistry studies<sup>22–24</sup> to the shock wave experiment of Mimura<sup>25</sup> and the laser ablation experiment of graphite under different quenching atmospheres by Jäger et al.<sup>26</sup> Chemical reaction networks that model the formation of PAHs in combustion flames<sup>27–29</sup> and in the interstellar medium<sup>30</sup> stress the importance of the phenylacetylene molecule ( $C_6H_5CCH$ ) in the growth of PAHs starting from an initial hydrogen abstraction/acetylene addition sequence via the phenyl radical. Here, PAHs are suggested to be formed via “polymerization” of acetylene via the HACA mechanism (hydrogen abstraction acetylene addition) starting with the addition of a phenyl radical to acetylene<sup>27</sup> followed by acetylene additions eventually closing the secondary ring.<sup>31</sup> However, recent crossed beam studies<sup>32,33</sup> and electronic structure calculations<sup>34</sup> showed that the reaction of phenyl radicals ( $C_6H_5$ ) with acetylene ( $C_2H_2$ ), which leads to the synthesis of phenylacetylene, has an entrance barrier of  $16 \text{ kJ mol}^{-1}$ . This barrier can certainly be overcome in high temperature combustion flames, but not in the low temperature, hydrocarbon-rich atmosphere of Titan (80–160 K).<sup>35</sup>

Kinetics and theoretical investigations proposed an alternative pathway to the phenylacetylene molecule via the reaction of the ethynyl radical ( $C_2H$ ) with benzene ( $C_6H_6$ ). Recent kinetics studies of this system within a temperature range from 105 to 298 K depicted unambiguously that the reaction occurs without an entrance barrier and is near the classical gas kinetic limits with a suggested rate expression,  $k(T)$ , as  $k(T) = 3.38(\pm 1.0) \times 10^{-10}(T/298)^{-0.18(\pm 0.18)} \text{ cm}^3 \text{ molecule}^{-1} \text{ s}^{-1}$  with  $T$  being the temperature in Kelvin.<sup>36</sup> Since these studies only monitored the decay kinetics of the open shell species, the product(s) was/were unidentifiable. Also, recent ab initio studies by Landera et al.<sup>37</sup> and Woon<sup>38</sup> confirm that the reaction of ethynyl radical

\* Corresponding author. E-mail: ralfk@hawaii.edu.

<sup>†</sup> Department of Chemistry, University of Hawai'i at Manoa.

<sup>‡</sup> NASA Astrobiology Institute, University of Hawai'i at Manoa.

<sup>§</sup> Florida International University.

with benzene proceeds without an entrance barrier; two thermodynamically favored pathways were identified, leading ultimately to the formation of phenylacetylene on the  $C_8H_7$  potential energy surface. Both pathways involve the formation of an adduct via addition of the ethynyl radical to the benzene ring without entrance barriers. From this point, hydrogen migration may occur followed by hydrogen elimination. Alternatively, phenylacetylene may be formed from the adduct via hydrogen elimination. The only other exoergic product channel identified was the hydrogen abstraction pathway leading to the formation of acetylene and phenyl radical. However, this channel was shown to be insignificant at low temperatures as it involves a large barrier of  $184 \text{ kJ mol}^{-1}$ . Note that previous crossed molecular beam studies investigated elementary bimolecular reactions of ethynyl radicals with unsaturated hydrocarbons. Here, the reactions of ethynyl radicals with methylacetylene ( $CH_3CCH$ ) yielded two isomers: ethynylallene ( $H_2CCCH(C_2H)$ ) and methylacetylene ( $CH_3CCCCH$ ).<sup>39</sup> Bimolecular collisions with the allene ( $H_2CCCH_2$ ) isomer and with ethylene produce ethynylallene ( $H_2CCCH(C_2H)$ )<sup>40</sup> and vinylacetylene ( $C_2H_3CCH$ ), respectively.<sup>41</sup> Finally, ethynyl radical reactions with acetylene ( $C_2H_2$ ) and diacetylene formed highly unsaturated polyynes and their radicals: diacetylene ( $HCCCCH$ ) together with butadiynyl ( $HCCCC$ )<sup>42</sup> and triacetylene ( $HCCCCCCH$ ), respectively,<sup>43</sup> via an addition–elimination reaction mechanism. All initial addition steps proceeded without entrance barrier, and the overall reactions were exoergic. Accordingly, the ethynyl radical is expected to react with benzene under the low temperature conditions in the atmosphere of Titan. Most importantly, if proven correct, the formation of phenylacetylene via the barrierless reaction of ethynyl with benzene presents a strong alternative to the hitherto postulated reaction of phenyl radicals with acetylene as derived from mechanistical reaction networks of combustion flames. It is important to stress that the benzene molecule ( $C_6H_6$ )<sup>44–46</sup> is present in the atmosphere of Titan along with highly reactive ethynyl radicals ( $C_2H$ ); the latter are predominantly formed from the solar ultraviolet photolysis of acetylene at wavelengths below  $200 \text{ nm}$ .<sup>47–51</sup> Therefore, the present crossed beam study of the perdeutero variant of the ethynyl radical with benzene is aimed to extract the underlying chemical dynamics together with potential reaction intermediates and the final reaction product under single collision conditions to shed light if the phenylacetylene molecule can be formed via a barrierless reaction of benzene with the ethynyl radical.

## 2. Experimental and Data Analysis

The experiments were conducted in a universal crossed molecular beam machine under single collision conditions at the University of Hawai'i. The experimental setup has been described in detail elsewhere.<sup>52–55</sup> Briefly, a supersonic beam of deuterated ethynyl radicals,  $C_2D(X^2\Sigma^+)$ , was generated in the primary source via laser ablation of graphite at  $266 \text{ nm}$  and consecutive reaction of the ablated species with neat deuterium gas (99.995%; Icon). Deuterium also acted as a seeding gas of the ethynyl radicals. The deuterium gas was released by a Proch-Trickl pulsed valve operating with a  $0.5 \text{ mm}$  nozzle at  $60 \text{ Hz}$ ,  $80 \mu\text{s}$  pulse width,  $-500 \text{ V}$  pulse amplitude, and  $4 \text{ atm}$  backing pressure. The distance between the nozzle and the skimmer was  $36 \text{ mm}$ . Under these operating conditions, the pressure in the primary source was maintained at about  $4 \times 10^{-4} \text{ Torr}$ . The rotating carbon rod was mounted on an in-house built ablation source.<sup>56</sup> The  $266 \text{ nm}$  laser beam was focused by a  $1.5 \text{ m}$  quartz lens from the fourth harmonic ( $266 \text{ nm}$ ) output of a Spectra-

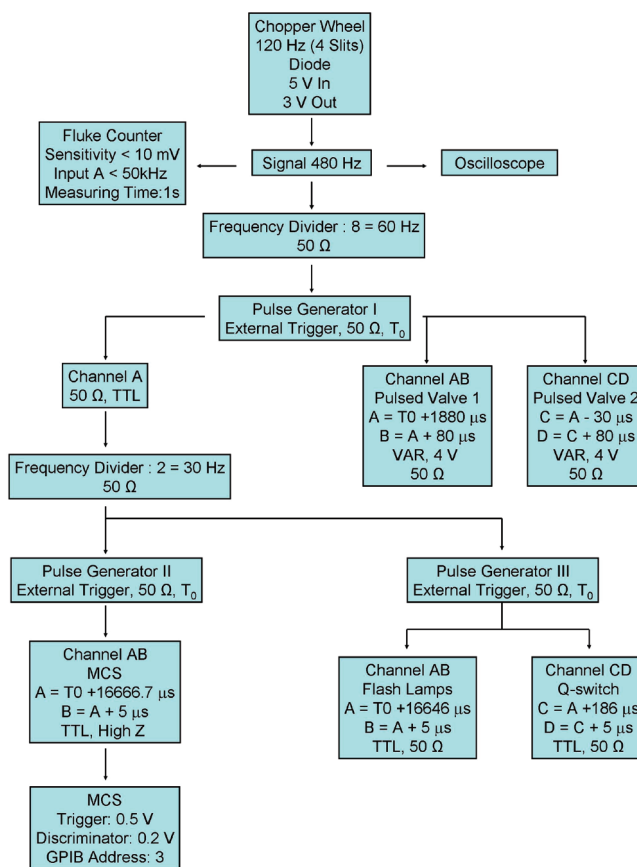


**Figure 1.** Timing sequence for the crossed molecular beam experiment of ethynyl- $d_1$  radicals [ $C_2D(X^2\Sigma^+)$ ] with benzene- $d_6$  [ $C_6D_6(X^1A_{1g})$ ].

Physics Quanta-Ray Pro 270 Nd:YAG laser operated at  $30 \text{ Hz}$  and  $20\text{--}25 \text{ mJ}$  per pulse to hit the carbon rod intersecting the deuterium beam perpendicularly about  $12\text{--}15 \text{ mm}$  downstream of the nozzle. The ethynyl- $d_1$  radicals were generated at the ablation center and carried in the deuterium beam. After the beam passed a skimmer, a four-slot chopper wheel selected a part of the ethynyl- $d_1$  beam at a peak velocity,  $v_p$  of  $2300 \pm 20 \text{ ms}^{-1}$  and a speed ratio,  $S$ , of  $5.0 \pm 0.3$ . The chopper wheel also acted as a timer to define the time zero in the experiments. Assisted by two frequency dividers (Pulse Research Lab, PRL-220A) and three pulse generators (Stanford Research System, DG535), a photodiode mounted on top of the chopper wheel provided the time zero trigger to control the experiment (Figure 1). The traveling time of the primary beam between the ablation center and interaction region was about  $20 \mu\text{s}$ . Since the lifetime of the  $A^2A'$  state is less than  $1 \mu\text{s}$ , any electronically excited  $C_2D(A^2A')$  species would relax while traveling from the ablation center to the interaction region. The chopped  $C_2D(X^2\Sigma^+)$  segment of the ethynyl- $d_1$  beam crossed a pulsed benzene- $d_6$  beam seeded in neon from the secondary source. Briefly, by passing  $750 \text{ Torr}$  of neon gas (Ne, 99.999%, Gaspro) through benzene- $d_6$  ( $C_6D_6$ , 99.5% D, Cambridge Isotope) stored in a stainless steel bubbler at  $293 \text{ K}$ , a 5% benzene- $d_6$ –neon mixture was obtained. This mixture was then released by a second pulsed valve  $30 \mu\text{s}$  prior to the primary pulsed valve in the secondary source to cross the ethynyl- $d_1$  beam perpendicularly in the interaction region. This pulsed valve operated with a  $1.0 \text{ mm}$  nozzle at  $60 \text{ Hz}$ ,  $80 \mu\text{s}$  pulse width,  $-500 \text{ V}$  pulse amplitude, and a nozzle–skimmer distance of  $14 \text{ mm}$ . The velocity and speed ratio of the benzene- $d_6$  beam were measured as  $750 \text{ ms}^{-1}$  and  $20$ , respectively. Thus, a collision energy of  $58.1 \pm 0.5 \text{ kJ mol}^{-1}$  was obtained. While the pulsed valve was operating, the

actual pressure in the secondary source was about  $5 \times 10^{-5}$  Torr. To optimize the intensity of each supersonic beam, which strongly depends on the distance between the pulsed valve and the skimmer, on line and in situ, each pulsed valve was placed on an ultrahigh vacuum compatible micropositioning translation stages with three stepper motors (New Focus). This allows monitoring the beam intensity versus the position of the pulsed valve in each source chamber in real time. It should also be noted that the primary reactant beam also contains carbon atoms as well as dicarbon and tricarbon molecules. Previous studies showed that tricarbon molecules have a significant entrance barrier upon reacting with benzene of more than  $90 \text{ kJ mol}^{-1}$ ;<sup>57</sup> therefore, under our experimental conditions, tricarbon does not react with benzene-*d*<sub>6</sub>. The lighter carbon (12 amu) and dicarbon reactants (24 amu) react with benzene-*d*<sub>6</sub>,<sup>58,59</sup> due to the heavier ethynyl-*d*<sub>1</sub> radical (26 amu), carbon and dicarbon reactions lead only to products, which are lower in mass by 2 and 14 amu compared to those formed in the reaction of ethynyl-*d*<sub>1</sub> radicals with benzene-*d*<sub>6</sub>. Consequently, neither dicarbon nor carbon atoms interfered in the present study.

The reactively scattered products were monitored by a triply differentially pumped quadrupole mass spectrometric detector operated in the time-of-flight (TOF) mode at a constant mass-to-charge ratio (*m/z*) after electron-impact ionization of the molecules at 80 eV at an emission current of 2 mA. These charged particles were then separated by an Extrel QC 150 quadrupole mass spectrometer operated with an oscillator at 2.1 MHz; only ions with a desired mass-to-charge, *m/z*, value passed through and were accelerated toward a stainless steel target coated with an aluminum layer and operated at a voltage of  $-22.5 \text{ kV}$ . The ions hit the surface and initiated an electron cascade that was accelerated by the same potential until they reached an aluminum coated organic scintillator whose photon cascade was detected by a photomultiplier tube (PMT, Burle, Model 8850, operated at  $-1.35 \text{ kV}$ ). The signal from the PMT was then filtered by a discriminator (Advanced Research Instruments, Model F-100TD, level: 1.4 mV) prior to feeding into a Stanford Research System SR430 multichannel scaler to record time-of-flight spectra.<sup>53,54</sup> Up to  $2.6 \times 10^6$  TOF spectra were recorded at each angle. The detector is rotatable within the plane defined by the ethynyl-*d*<sub>1</sub> radical and benzene-*d*<sub>6</sub> beams; this allows recording angular resolved TOF spectra and, by integrating the TOF spectra at the laboratory angles, the laboratory angular distribution. The latter reports the integrated intensity of an ion of distinct *m/z* versus the laboratory angle. To gain additional information on the chemical dynamics and underlying reaction mechanism, the TOF spectra and laboratory angular distribution were fit and transformed into the center-of-mass reference frame using a forward-convolution routine.<sup>60,61</sup> This approach initially presumes the angular flux distribution  $T(\theta)$  and the translational energy flux distribution  $P(E_T)$  in the center-of-mass system (CM) assuming mutual independence. The laboratory data (TOF spectra and the laboratory angular distribution) are then calculated from these  $T(\theta)$  and  $P(E_T)$  and convoluted over the apparatus functions to obtain a simulation of the experimental data. The crucial output of this fitting routine is the product flux contour map,  $I(\theta, u) = P(u) \times T(\theta)$ , which plots the intensity of the reactively scattered products (*I*) as a function of the center-of-mass scattering angle ( $\theta$ ) and product velocity (*u*). This plot is called the reactive *differential cross section* and can be seen as the *image* of the chemical reaction.

### 3. Results

**3.1. Laboratory Data.** The reactive scattering signal for the reaction of the deuterated ethynyl radical [ $\text{C}_2\text{D}(\text{X}^2\Sigma^+)$ ] with

benzene-*d*<sub>6</sub> [ $\text{C}_6\text{D}_6(\text{X}^1\text{A}_{1g})$ ] was monitored at a mass-to-charge ratio (*m/z*) of 108 ( $\text{C}_8\text{D}_6^+$ ) and with benzene [ $\text{C}_6\text{H}_6(\text{X}^1\text{A}_{1g})$ ] at *m/z* = 103 ( $\text{C}_8\text{H}_5\text{D}^+$ ). These ions correspond to the parent ions and also to the most intense mass fragment. Due to the high background level at *m/z* = 28 (from background carbon monoxide in the detector), no discernible signal was detected from the hydrogen abstraction reaction to form the deuterated acetylene ( $\text{C}_2\text{D}_2$ ) product plus the phenyl-*d*<sub>5</sub> radical [ $\text{C}_6\text{D}_5$ ]. Similarly, the background at *m/z* = 82 [ $\text{C}_6\text{D}_5^+$ ] was too high due to the electron impact fragmentation of the benzene-*d*<sub>6</sub> [ $\text{C}_6\text{D}_6(\text{X}^1\text{A}_{1g})$ ] parent molecule. These data have important implications. The detection of  $\text{C}_8\text{D}_6$  in the reaction of benzene-*d*<sub>6</sub> with the ethynyl-*d*<sub>1</sub> radical suggests the presence of an ethynyl-*d*<sub>1</sub> addition followed by an atomic deuterium elimination pathway. However, the deuterium atom could leave the adduct from the benzene ring or from the ethynyl-*d*<sub>1</sub> radical. To discriminate these options, the results from the ethynyl-*d*<sub>1</sub> plus benzene experiments are advantageous. Here, the signal at *m/z* = 103 ( $\text{C}_8\text{H}_5\text{D}^+$ ) indicates that the deuterium atom at the ethynyl-*d*<sub>1</sub> unit stays in the product molecule and that the hydrogen atom is emitted from the benzene ring. The lack of signal at *m/z* = 102 ( $\text{C}_8\text{H}_4\text{D}^+/\text{C}_8\text{H}_6^+$ ) for the benzene-ethynyl-*d*<sub>1</sub> radical is interesting. First, it shows that the reaction of ethynyl-*d*<sub>1</sub> with benzene does not lead to the emission of a deuterium atom leading to a product of the generic formula  $\text{C}_8\text{H}_6$ . Second, the molecular hydrogen elimination forming  $\text{C}_8\text{H}_4\text{D}$  is also negated. Also, that no signal was observed at *m/z* = 102 is in agreement with the mass fragment pattern of phenylacetylene, as reported in the NIST database;<sup>62</sup> i.e., only 2% of the parent ion will fragment via hydrogen bond rupture, which is well within the noise of the experimental apparatus. A comparison of the TOF spectra collected at the center-of-mass angle of  $45.25^\circ$  for products with *m/z* ratios of 103 ( $\text{C}_8\text{H}_5\text{D}^+$ ) and 102 ( $\text{C}_8\text{H}_4\text{D}^+/\text{C}_8\text{H}_6^+$ ) amu is shown in Figure 2.

Selected time-of-flight profiles are shown in Figure 3 along with the calculated temporal distributions derived from the forward-convolution fitting routine as mentioned above. A key point to be stressed is that the TOF profiles were successfully replicated with only one product channel with mass combinations of 108 amu (deuterated phenylacetylene;  $\text{C}_6\text{D}_5\text{CCD}$ ) and 2 amu (deuterium atom, D). The corresponding laboratory angular distribution (LAB) is shown in Figure 4 with the optimal curve derived from the best fit center-of-mass functions. An inspection of the LAB distribution suggests that the LAB distribution is forward-backward symmetric and peaks at the center of mass angle. The shape of this LAB distribution indicates that the reaction proceeds via indirect scattering dynamics involving  $\text{C}_8\text{D}_7$  intermediate(s).

**3.2. Center of Mass Functions.** The center-of-mass angular,  $T(\theta)$ , and translational energy,  $P(E_T)$ , distributions that yielded the best fit in the laboratory frame for products of the mass combination 108 amu ( $\text{C}_8\text{D}_6$ ) and 2 amu (atomic deuterium) are shown in Figure 5. Let us investigate the center-of-mass translational energy distribution first. The reaction exoergicity is reflected in the translational energy distribution. For those product molecules not internally excited, the *maximum translational energy*,  $E_{\text{max}}$ , allowed is the arithmetic sum of the collision energy and the absolute of the reaction exoergicity. Accordingly, the reaction exoergicity can be determined by subtracting the collision energy from the maximum translational energy,  $E_{\text{max}}$ , observed. Within the experimental error limits, this yields a reaction exoergicity of  $121 \pm 10 \text{ kJ mol}^{-1}$ . This value is in direct agreement to those derived from ab initio electronic structure calculations<sup>37</sup> of  $111 \pm 10 \text{ kJ mol}^{-1}$  and

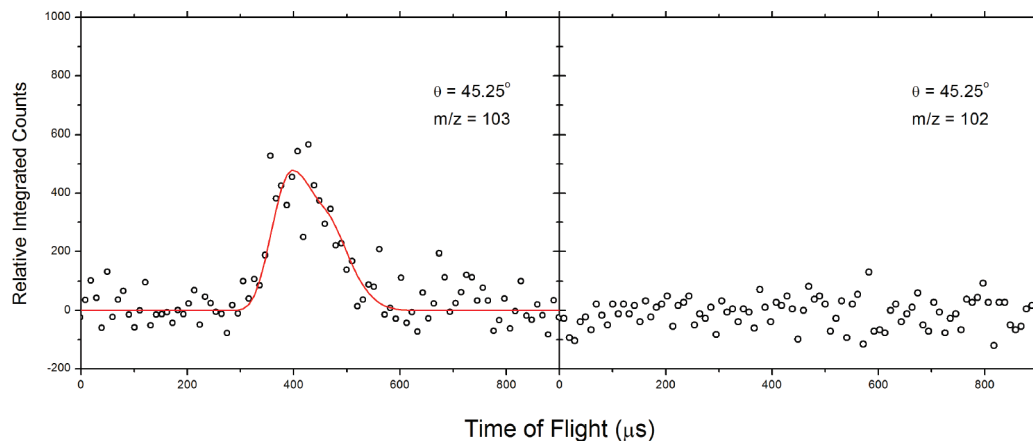


**Figure 2.** Time-of-flight spectra for two ions recorded at the center-of-mass angle  $45.25^\circ$  at  $m/z = 103$  and  $102$  for the reaction of the ethynyl- $d_1$  [ $C_2D(X^2\Sigma^+)$ ] radical with benzene [ $C_6H_6(X^1A_{1g})$ ]. The signal at  $m/z = 103$  originates from ionized  $C_8H_5D$ ; no signal at  $m/z = 102$  was observed. In principle, the signal at  $m/z = 102$  could originate from the molecular hydrogen elimination channel leading to  $C_8H_4D$ , from the atomic deuterium elimination pathway forming  $C_8H_6$ , and/or from dissociative ionization of  $C_8H_5D$ . Open circles represent the experimental data; the solid red lines, the fits.

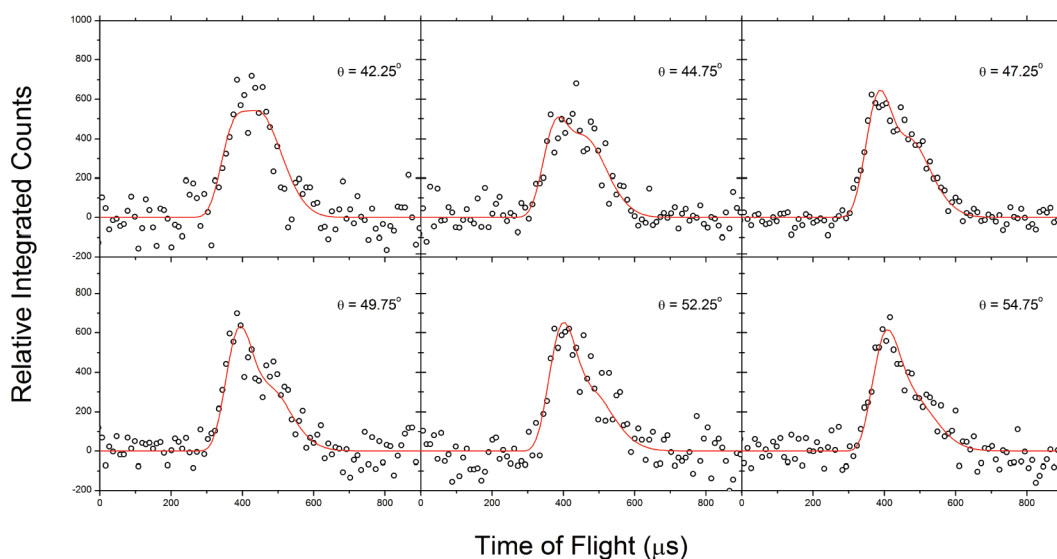


**Figure 3.** Time-of-flight spectra of the ionized reaction product monitored at  $m/z = 84$  formed in the reaction of ethynyl- $d_1$  [ $C_2D(X^2\Sigma^+)$ ] with benzene- $d_6$  [ $C_6D_6(X^1A_{1g})$ ]. Open circles signify the experimental data. Solid red lines represent the calculated distribution of the phenylacetylene- $d_6$  ( $C_6D_5CCD$ ) product.

from standard enthalpy values taken from the NIST database.<sup>62</sup> Second, the translational energy distribution peaks well away from zero translational energy at about  $44 \text{ kJ mol}^{-1}$ . This finding indicates that the exit transition state is likely to be tight;<sup>63</sup> further, this process involves a significant electron rearrangement from the decomposing intermediate to the final phenylacetylene- $d_6$  plus deuterium atom products. The translational energy distribution also allows for the determination of the percentage of available energy partitioned into the rotational and vibrational degrees of freedom. This value was determined to be about  $53 \pm 6\%$  of the available energy.

The center-of-mass angular distribution reveals important additional information on the reaction dynamics. Upon first inspection, one would notice that the intensity of the center-of-mass angular distribution is always greater than zero for all angles. This finding implies indirect scattering dynamics via a  $C_8D_7$  intermediate. Second, the angular distribution is forward-backward symmetric about  $90^\circ$ . The symmetry suggests that the intermediate has a lifetime longer than the rotational period of the decomposing complex.<sup>64,65</sup> The ratios of the flux intensities at the respective maxima and minima,  $I(90^\circ)/I(0^\circ)$ , were

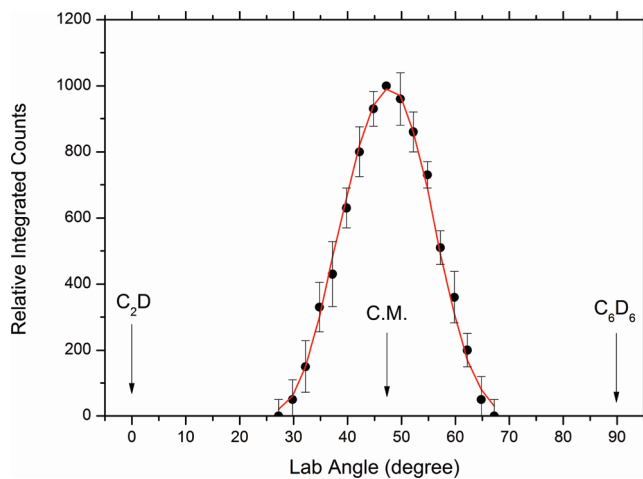


**Figure 4.** Laboratory angular distribution for the reaction of ethynyl- $d_1$  [ $C_2D(X^2\Sigma^+)$ ] with benzene- $d_6$  [ $C_6D_6(X^1A_{1g})$ ]; the product is monitored at  $m/z = 108$  ( $C_8D_6^+$ ). Solid circles represent the experimental data together with  $1\sigma$  error bars. The solid red line corresponds to the calculated distribution for the phenylacetylene- $d_6$  product ( $C_6D_5CCD$ ). C.M. designates the center-of-mass angle.

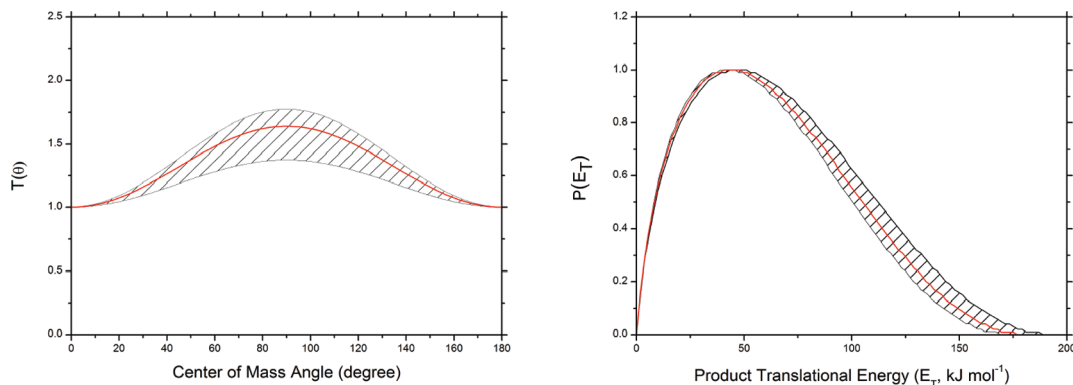


**Figure 5.** Center-of-mass angular (left) and translational energy flux distribution (right) of the phenylacetylene- $d_6$  ( $C_6D_5CCD$ ) product observed in the reaction of ethynyl- $d_1$  radicals  $C_2D(X^2\Sigma^+)$  with benzene- $d_6$  [ $C_6D_6(X^1A_{1g})$ ] at a collision energy of  $58.1 \text{ kJ mol}^{-1}$ . Hatched areas indicated the acceptable upper and lower error limits of the fits. The solid red line defines the best fit function for the phenylacetylene- $d_6$  product.

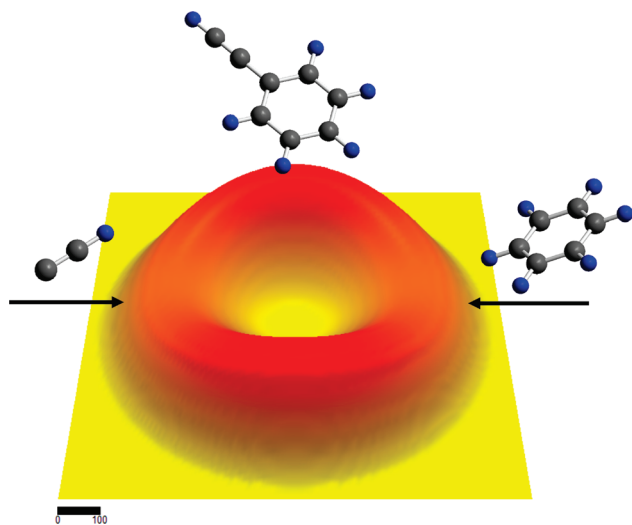


**Figure 6.** Flux contour map derived from the best fit center-of-mass functions for the phenylacetylene- $d_6$  product formed in the reaction of ethynyl- $d_1$  radicals [ $C_2D(X^2\Sigma^+)$ ] with benzene- $d_6$  [ $C_6D_6(X^1A_{1g})$ ] at a collision energy of  $58.1 \text{ kJ mol}^{-1}$ , the scale is in units of  $\text{ms}^{-1}$ .

found to be  $1.64 \pm 0.2$ . This “sideways scattering” reveals the geometrical constraints of the decaying intermediate; here, the deuterium atom is ejected perpendicular to the molecular rotational plane almost parallel to the total angular momentum vector.<sup>64,66</sup> These characteristics are also revealed in the flux contour map, as shown in Figure 6. Here, the flux distribution is forward–backward symmetric and shows a sideways-scattering pattern.

#### 4. Discussion

As verified from a comparison of the experimental data with literature values, the high energy cutoff of the center-of-mass translation energy distribution,  $P(E_T)$ , is in direct agreement with both values based upon ab initio calculations<sup>37</sup> and basic enthalpy considerations taken from the NIST database<sup>62</sup> to form the phenylacetylene- $d_6$  isomer ( $C_6D_5CCD$ ) plus atomic deuterium in a strongly exoergic reaction ( $121 \pm 10 \text{ kJ mol}^{-1}$ ). Note that previous electronic structure calculations<sup>37,38</sup> predicted multiple thermodynamically stable  $C_8H_6$  isomers such as cyclic  $C_8H_6$ . However, among all the possible isomers synthesized, the only molecule formed in the ethynyl- $d_1$  plus benzene- $d_6$  reaction via an exoergic process was the phenylacetylene- $d_6$  species. Besides the ethynyl- $d_1$  versus deuterium exchange pathway to form the phenylacetylene- $d_6$  molecule, the only other

exoergic channel was the deuterium abstraction to form acetylene- $d_2$  plus the phenyl- $d_5$  radical. As outlined in the experimental section, this pathway could not be traced. Calculations by both Landera<sup>37</sup> et al. and Woon<sup>38</sup> concluded that this channel is not significant. Landera et al. determined that the deuterium abstraction channel must proceed via a roaming mechanism with a significant exit barrier of about  $184 \text{ kJ mol}^{-1}$ . This is clearly above our collision energy and also above the equivalent temperature in Titan’s atmosphere. Thus, the abstraction reaction pathway does not compete with the formation of phenylacetylene- $d_6$ . To summarize, on the basis of the energetics of the reaction and the comparison with NIST data and electronic structure calculations, the phenylacetylene molecule along with atomic deuterium are concluded to be the primary products.

How can the phenylacetylene- $d_6$  molecule be formed? Recall that both the center-of-mass angular distribution and the fraction of energy channeling into the translational modes of the products suggest an indirect reaction mechanism via complex formation; this  $C_8D_7$  reaction intermediate was found to be long-lived compared to its rotational period. Further, the decomposing complex fragmented via deuterium emission involving a tight exit transition state on the order of about  $42 \text{ kJ mol}^{-1}$ . In other words, the reversed reaction of an addition of the deuterium atom to the phenylacetylene- $d_6$  molecule has an entrance barrier. This is consistent with addition of a hydrogen/deuterium atom to a closed shell, unsaturated moiety of the molecule such as double, triple, or “aromatic” bonds. Finally, data with benzene suggest that the deuterium atom of the ethynyl- $d_1$  molecule stays intact, and that a hydrogen atom is eliminated from the benzene ring. On the basis of these findings, we propose that the ethynyl- $d_1$  radical adds to the benzene- $d_6$  molecule to form a  $C_6D_6CCD$  intermediate, the latter fragmenting via atomic deuterium loss, forming the phenylacetylene- $d_6$  molecule. These findings and the suggested reaction mechanism gain full support from the computed potential energy surfaces (Figure 7) adapted from Landera et al.<sup>37</sup> In this figure, only the pathways leading to the formation of phenylacetylene are shown. It should be stressed that our reaction was conducted with ethynyl- $d_1$  and benzene- $d_6$ . Consequently, the pathways relevant to the reaction dynamics on the formation of phenylacetylene have been recalculated to account for the difference in the zero point energy. The computational methods employed were described in ref 37. As seen in Figure 7, two reaction pathways are possible. Both begin with the formation of an adduct without an entrance barrier forming the reactive intermediate **i1**. From **i1**, the reaction may proceed through a hydrogen migration via **TS2** to form intermediate **i2** followed by hydrogen atom elimination through

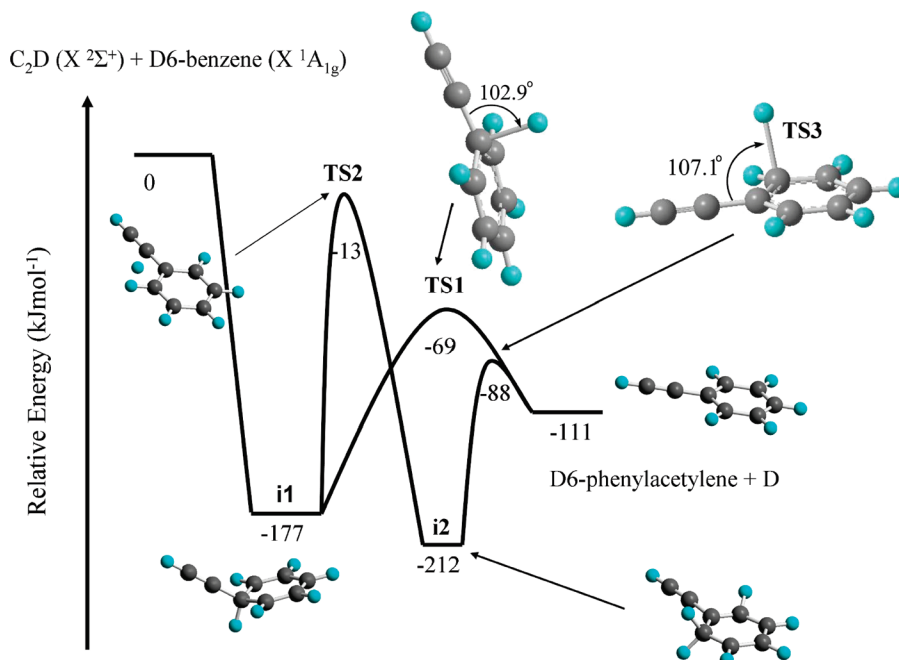


**Figure 7.** Potential energy surface for the reaction of ethynyl radical [ $C_2D(X\ 2\Sigma^+)$ ] with benzene- $d_6$  [ $C_6D_6(X\ 1A_{1g})$ ] adapted from ref 37, with zero point energy corrections.

transition state **TS3** with an exit barrier of 23  $\text{kJ mol}^{-1}$ . Alternatively, from reactive intermediate **i1**, phenylacetylene may be produced via hydrogen atom loss through transition state **TS1**. Considering the reverse of this reaction, a barrier for addition of a hydrogen atom to the carbon atom was determined to be 42  $\text{kJ mol}^{-1}$ . This agrees adequately with our experimental findings. Also, considering the geometry of the exit transition states (**TS1**, **TS3**) the attacking hydrogen atom is oriented almost perpendicularly to the molecular plane of phenylacetylene at angles of 102.9° and 107.1°, respectively. Consequently, from the center of mass laboratory angular distribution, both pathways may contribute to the overall formation of phenylacetylene. However, due to the peak of the center-of-mass translational energy distribution at about 40  $\text{kJ mol}^{-1}$ , the pathway most dominant is suggested to be one through **TS1**, via a hydrogen atom elimination. Finally, we would like to comment on the “sideways patterns” found experimentally. Here, the overall shape of  $T(\theta)$  is dictated by the disposal of the total angular momentum **J**. One of the consequences of the pulsed supersonic expansion used in the experiment is the rotational cooling of the reactant molecules. Accordingly, the total angular momentum can be approximated by assuming that only the initial orbital angular momentum **L** will play a considerable role. Taking into consideration angular momentum conservation, the initial orbital angular momentum **L** must be identical to the sum of the final orbital angular momentum **L'** and rotational momentum **j'**. The final recoil velocity vector of the product **v'** will be in the plane perpendicular to **L'**. Consequently, when rotational excitation of the products is significant, the velocity vector of the product will be almost parallel to **J**.<sup>66</sup> As shown in Figure 5,  $T(\theta)$  reveals a sideways scattering pattern, suggesting that the H(D) atom is ejected almost perpendicularly to the molecular plane of the reactive intermediate, as predicted in the  $C_8H_7$  potential energy surface (Figure 7) at angles of 102.9° and 107.1°. This can also be verified by considering the reverse reaction, the deuterium atom attacking perpendicular to the molecular plane of phenylacetylene. Similar to the addition of a hydrogen atom to the aromatic benzene molecule, where an entrance barrier of 27  $\text{kJ mol}^{-1}$  is found,<sup>67</sup> this process is expected to have an entrance

barrier. The existence of an entrance barrier for the reversed reaction, i.e., the addition of the deuterium atom to the phenylacetylene molecule, is well reflected in the distribution maximum of the center-of-mass translational energy distribution,  $P_{\max}(E)$ , of 38.7–45.7  $\text{kJ mol}^{-1}$ .

Considering that the cyano radical (CN;  $X\ 2\Sigma^+$ ) and the ethynyl radical are isoelectronic and both radicals have been shown to be important reactive species in Titan's atmosphere,<sup>68</sup> a brief comparative summary of their dynamics is given here. First, both reactions are initiated by a barrierless addition of the radical R to the benzene- $d_6$  molecule, forming a reaction intermediate of the generic formula  $C_6D_6R$ ; at collision energies of 58.1  $\text{kJ mol}^{-1}$  (R = ethynyl- $d_1$ ) and 19.5–34.4  $\text{kJ mol}^{-1}$  (R = CN), both intermediates are long-lived and stabilized by 177 and 165  $\text{kJ mol}^{-1}$  with respect to their separate reactants. Likewise, both intermediates decompose via atomic deuterium loss through tight exit transition states located 42 and 33  $\text{kJ mol}^{-1}$  above the separated products, but below the total energy of the separated reactants. The amount of available energy partitioned into the translational degrees of freedom of  $C_6H_5CN$  was found to be 30–35%, whereas the title reaction illustrated a value of 53%. The discrepancy may be explained by the difference in collision energies at which both of the experiments were conducted. The title reaction was conducted at a significantly higher collision energy, leading to a shorter lifetime of the intermediate and hence less complete energy randomization in the vibration modes. The overall reactions to form phenylacetylene- $d_6$  and cyanobenzene- $d_5$  ( $C_6D_5CN$ ) were determined to be exoergic by  $121 \pm 10$  and  $88 \pm 8$   $\text{kJ mol}^{-1}$ . Finally, both center-of-mass angular distributions were found to be sideways peaked, indicating that in the decomposing complex, the deuterium atom was emitted perpendicularly to the rotation plane of the intermediate almost parallel to the total orbital angular momentum vector. These findings were supported by electronic structure calculations where, in regard to the decomposing intermediate for  $C_6H_6CN$ , the H–C–C bond angle was determined to be 101.2° and for **TS1** and **TS3** on the  $C_8H_7$  potential energy surface as shown in Figure 7 to be 102.9° and 107.1°.

## 5. Conclusion

We have conducted crossed molecular beam experiments of the deuterated ethynyl radical molecules in their  $X^2\Sigma^+$  electronic ground state with benzene and its fully deuterated analog at a collision energy of 58.1 kJ mol<sup>-1</sup>. This experiment was compared with a novel electronic structure calculation on the singlet C<sub>8</sub>D<sub>7</sub> surface. Phenylacetylene-*d*<sub>6</sub> is the primary product formed via indirect reactive scattering dynamics through a long-lived reaction intermediate initiated by a barrierless addition of the ethynyl-*d*<sub>1</sub> radical to benzene-*d*<sub>6</sub>. This initial intermediate was found to decompose via a tight exit transition state located about 42 kJ mol<sup>-1</sup> above the separated products; here, the deuterium atom is ejected almost perpendicularly to the rotational plane of the decomposing intermediate and almost parallel to the total angular momentum vector. The overall exoergicity of the reaction is shown to be 121 ± 10 kJ mol<sup>-1</sup>. Observation of rate constants by Goulay et al.<sup>36</sup> also depicted that the reaction of the ethynyl radical with benzene is very rapid within gas kinetics even at low temperatures present on Titan. Therefore, we can conclude that the reaction of ethynyl radicals with benzene can form the phenylacetylene molecule in the atmosphere of Titan.

**Acknowledgment.** This work was supported in part by Chemistry Division of the U.S. National Science Foundation within the Collaborative Research in Chemistry Program (NSF-CRC CHE-0627854) (F.Z., P.M., R.I.K., A.M.M.) and was supported in part by an appointment to the NASA Postdoctoral Program at the NASA Astrobiology Institute, administered by Oak Ridge Associated Universities through a contract with NASA (B.J.).

## References and Notes

- Finlayson-Pitts, B. J.; Pitts, J. N. *Science* **1997**, *276*, 1045.
- Hylland, K. *J. Toxicol. Environ. Health Part A* **2006**, *125*, 054302.
- Violi, A.; Venkatnathan, A. *J. Chem. Phys.* **2006**, *125*, 054302–8.
- Seinfeld, J. H.; Pankow, J. F. *Annu. Rev. Phys. Chem.* **2003**, *54*, 121.
- Kazakov, A.; Frenklach, M. *Combust. Flame* **1998**, *112*, 270.
- Pendleton, Y. J.; Allamandola, L. J. *Astrophys. J. Suppl. Ser.* **2002**, *138*, 75.
- Peeters, E.; Mattioda, A. L.; Hudgins, D. M.; Allamandola, L. J. *Astrophys. J.* **2004**, *617*, L65.
- Solid State Astrochemistry*; Valerio Pirronello, J. K., Giulio, Manicò, Eds.; Kluwer Academic Publishers: Norwell, 2003.
- Duley, W. W. *Faraday Discuss.* **2006**, *133*, 415–425.
- Ruiterkamp, R.; Halasinski, T.; Salama, F.; Foing, B. H.; Allamandola, L. J.; Schmidt, W.; Ehrenfreund, P. *Astron. Astrophys.* **2002**, *390*, 1153–1170.
- Ehrenfreund, P.; Foing, B. H. *Planet. Space Sci.* **1995**, *43*, 1183–1187.
- Ehrenfreund, P.; Sephton, M. A. *Faraday Discuss.* **2006**, *133*, 277–288.
- Yung, Y. L.; Allen, M.; Pinto, J. P. *Astrophys. J., Suppl. Ser.* **1984**, *55*, 465.
- Letourneur, B.; Coustenis, A. A. *Planet. Space Sci.* **1993**, *41*, 593.
- Hidayat, T.; Marten, A.; Bezaud, B.; Gautier, D.; Owen, T.; Matthews, H. E.; Paubert, G. *Icarus* **1998**, *133*, 109.
- Marcus, R. A. *J. Chem. Phys.* **2004**, *121*, 8201.
- Clarke, D. W.; Ferris, J. P. *Icarus* **1997**, *127*, 158.
- Hidayat, T.; Marten, A.; Bezaud, B.; Gautier, D.; Owen, T.; Matthews, H. E.; Paubert, G. *Icarus* **1997**, *126*, 170.
- Lunine, J. I.; Yung, Y. L.; Lorenz, R. D. *Planet. Space Sci.* **1999**, *47*, 1291.
- Gurwell, M. A. *Astrophys. J.* **2004**, *616*, L7.
- Wong, A.-S.; Morgan, C. G.; Yung, Y. L.; Owen, T. *Icarus* **2002**, *155*, 382.
- Burtscher, H. *J. Aerosol Sci.* **1992**, *23*, 549–595.
- Weilmünster, P.; Keller, A.; Homann, K. H. *Combust. Flame* **1999**, *116*, 62–83.
- Dobbins, R. A.; Fletcher, R. A.; Chang, H. C. *Combust. Flame* **1998**, *115*, 285–298.
- Mimura, K. *Geochim. Cosmochim. Acta* **1994**, *59*, 579–591.
- Jaeger, C.; Huisken, F.; Mutschke, H.; Llamas Jansa, I.; Henning, T. *arXiv.org, e-Print Arch., Astrophys.* **2009**, 1–7, arXiv:0903.0775v1 [astro-ph GA].
- Wang, H.; Frenklach, M. *Combust. Flame* **1997**, *110*, 173–221.
- Appel, J.; Bockhorn, H.; Frenklach, M. *Combust. Flame* **2000**, *121*, 122.
- Richter, H.; Howard, J. B. *Phys. Chem. Chem. Phys.* **2002**, *4*, 2038.
- Frenklach, M.; Feifelson, E. D. *Astrophys. J.* **1989**, *341*, 372.
- Bittner, J. D.; Howard, J. B. *Symp. (Int.) Combust.* **1981**, *18*, 1105–1116.
- Xibin Gu, F. Z.; Ying, Guo; Kaiser, R. I. *Angew. Chem., Int. Ed. Engl.* **2007**, *46*, 6866–6869.
- Gu, X.; Kaiser, R. I. *Acc. Chem. Res.* **2008**, *42*, 290–302.
- Tokmakov, I. V.; Lin, M. C. *J. Am. Chem. Soc.* **2003**, *125*, 11397–11408.
- Flasar, F. M.; et al. *Science* **2005**, *308*, 975–978.
- Goulay, F.; Leone, S. R. *J. Phys. Chem. A* **2006**, *110*, 1875–1880.
- Landera, A.; Mebel, A. M.; Kaiser, R. I. *Chem. Phys. Lett.* **2008**, *459*, 54–59.
- Woon, D. E.; Park, J.-Y. *Icarus* **2009**, *202*, 642–655.
- Kaiser, R. I.; Chiong, C. C.; Asvany, O.; Lee, Y. T.; Stahl, F.; Schleyer, P. v. R.; Schaefer, H. F., III. *J. Chem. Phys.* **2001**, *114*, 3488–3496.
- Zhang, F.; Kim, S.; Kaiser, R. I. *Phys. Chem. Chem. Phys.* **2009**, *11*, 4707–4714.
- Zhang, F.; Kim, Y. S.; Kaiser, R. I.; Krishtal, S. P.; Mebel, A. M. *J. Phys. Chem. A* **2009**, *113*, 11167–11173.
- Kaiser, R. I.; Stahl, F.; Schleyer, P. v. R.; Schaefer, H. F., III. *Phys. Chem. Chem. Phys.*, *4*, 2950–2958.
- Gu, X.; Kim, Y. S.; Kaiser, R. I.; Mebel, A. M.; Liang, M. C.; Yung, Y. L. *Proc. Natl. Acad. Sci.* **2009**, *106*, 16078–16083.
- Coustenis, A.; et al. *Icarus* **2003**, *161*, 383.
- Neimann, H.; et al. *Nature* **2005**, *438*, 779.
- Coustenis, A.; et al. *Icarus* **2007**, *189*, 35.
- Jackson, W. M.; Scodinu, A. *Astrophys. Space Sci. Lib.* **2004**, *311*, 85.
- Seki, K.; Okabe, H. *J. Phys. Chem.* **1993**, *97*, 5284.
- Balko, B. A.; Zhang, J.; Lee, Y. T. *J. Chem. Phys.* **1991**, *94*, 7958.
- Lauter, A.; Lee, K. S.; Jung, K. H.; Vatsa, R. K.; Mittal, J. P.; Volpp, H.-R. *Chem. Phys. Lett.* **2002**, *358*, 314.
- Gazeau, M. C.; Cottin, H.; Vuitton, V.; Smith, N.; Raulin, F. *Planet. Space Sci.* **2000**, *48*, 437–445.
- Guo, Y.; Gu, X.; Kaiser, R. I. *Int. J. Mass Spectrom.* **2006**, *249/250*, 420–425.
- Guo, Y.; Gu, X.; Kawamura, E.; Kaiser, R. I. *Rev. Sci. Instrum.* **2006**, *77*, 034701/1–034701/9.
- Gu, X. B.; Guo, Y.; Kawamura, E.; Kaiser, R. I. *Rev. Sci. Instrum.* **2005**, *76*, 083115/1–083115/6.
- Gu, X.; Guo, Y.; Kaiser, R. I. *Int. J. Mass Spectrom.* **2005**, *246*, 29–34.
- Gu, X.; Guo, Y.; Kawamura, E.; Kaiser, R. I. *J. Vac. Sci. Technol., A* **2006**, *24*, 505–511.
- Gu, X.; Guo, Y.; Mebel, A. M.; Kaiser, R. I. *Chem. Phys. Lett.* **2007**, *449*, 44–52.
- Hahndorf, I.; Lee, Y. T.; Kaiser, R. I.; Vereecken, L.; Peeters, J.; Bettinger, H. F.; Schreiner, P. R.; Schleyer, P. v. R.; Allen, W. D.; Schaefer, H. F., III. *J. Chem. Phys.* **2002**, *116*, 3248–3262.
- Gu, X.; Guo, Y.; Zhang, F.; Mebel, A. M.; Kaiser, R. I. *Chem. Phys. Lett.* **2007**, *436*, 7–14.
- Vernon, M. *Ph.D. Thesis*, University of California, Berkeley, 1981.
- Weiss, M. S. *Ph.D. Thesis*, University of California, Berkeley, 1986.
- National Institute of Standards and Technology. In *NIST Standard Reference Database Number 69*; Linstrom, P. J., Mallard, W. G., Eds.; NIST: Gaithersburg, MD.
- Kaiser, R. I.; Mebel, A. M. *Int. Rev. Phys. Chem.* **2002**, *21*, 307–356.
- Levine, R. D. *Molecular Reaction Dynamics*; Cambridge University Press: Cambridge, U.K., 2005.
- Miller, W. B.; Safron, S. A.; Herschbach, D. R. *Discuss. Faraday Soc.* **1967**, *44*, 108.
- Balucani, N.; Asvany, O.; Chang, A. H. H.; Lin, S. H.; Lee, Y. T.; Kaiser, R. I.; Bettinger, H. F.; Schleyer, P. v. R.; Schaefer, H. F., III. *J. Chem. Phys.* **1999**, *111*.
- Zhang, F.; Jones, B.; Maksyutenko, P.; Kaiser, R. I.; Chin, C.; Kislov, V. V.; Mebel, A. M. *J. Am. Chem. Soc.* **2010**, *132*, 2672–2683.
- Raulin, F.; Coll, P.; Coscia, D.; Gazeau, M. C.; Sternberg, R.; Brunton, P.; Israel, G.; Gautier, D. *Adv. Space Res.* **1998**, *22*, 353–362.